RSC Advances

ROYAL SOCIETY OF CHEMISTRY

www.rsc.org/advances

RSC Advances

COMMUNICATION

Improving the surface-enhanced Raman scattering activity of carbon nitride by two-step calcining

Received 00th January 20xx,
Accepted 00th January 20xx

DOI: 10.1039/x0xx00000x

www.rsc.org/

Jizhou Jiang*

We demonstrated a novel two-step calcining method for growing highly efficient surface-enhanced Raman scattering (SERS) substrates, modified g-C_3N_4. Their morphologies, microstructures and optical properties were successfully controlled by altering the calcining time. Moreover, the modified g-C_3N_4-2 h+Ag substrate exhibited superior SERS activity, suggesting its potential applications in SERS sensing.

Graphitic carbon nitride (g-C_3N_4) has attracted widespread attention due to its outstanding and unique chemical, catalytic and optical properties, along with its cheap, easily available, and remarkably high stability to oxidation, making it a very attractive material for water splitting,[1,2] photocatalytic,[3,4] organic catalytic[5-7] and electrocatalytic[8,9] applications. Commonly, for inorganic nanocatalysts, the size and crystal facets could significantly affect their catalytic performance. However, for carbon and g-C_3N_4 based catalysts, the morphology, microstructure and structural defects usually dominate their property and catalytic activity. Therefore, to manipulate the g-C_3N_4 catalytic and electronic performance, modifications of the g-C_3N_4 synthesis have been studied intensively.

Recently, Antonietti's group reported that the use of organic molecules like barbituric acid or molecules, which lead to integration of heteroatoms within g-C_3N_4 structure, can arouse significant changes in the electronic and catalytic properties.[10] Using a cyanuric acid-melamine complex in ethanol as a precursor, Shalom and co-workers prepared a pancake-like hollow g-C_3N_4 structures, which exhibited superior photocatalytic activity compared to the bulk material.[3] Nevertheless, the obtained samples were disorganized textures with small grain sizes, or the process was less controlled. Meanwhile, in our previously work,[11] the g-C_3N_4 was directly prepared by polymerization of melamine and the g-C_3N_4+Ag hybrid substrate exhibited a strong SERS response, but the g-C_3N_4+Ag hybrid substrate itself had a strong Raman signal which could interfere with the SERS detection of probe molecules. Therefore, it is essential to find new and simple synthetic pathways to prepare optimal g-C_3N_4 structures with an improving SERS activity.

In this communication, the modified g-C_3N_4 substrates were simply prepared by a two-step calcining method. The morphologies, microstructures and optical properties of the modified g-C_3N_4 were comprehensively characterized. Moreover, the modified g-C_3N_4-2 h+Ag substrates showed superior SERS activity compared to g-C_3N_4+Ag substrates.

Firstly, the g-C_3N_4 was prepared by heating melamine to 520 ^oC at a rate of 10 K min^{-1} for 4 h under air atmosphere in a muffle furnace.[12] Then, the as-prepared yellow powder was further calcined in a chemical vapor deposition (CVD) furnace. Pure N_2 was introduced into the quartz tube at a flow rate of 50 sccm, and the pressure inside the tube was held constant at 1 atm. The furnace was gradually heated to 600 ^oC at a rate of 10 K min^{-1} and held for different time. After cooling to room temperature, a fluffy powder was obtained. The products with different calcining time in the CVD furnace were referred to two-step calcining samples, g-C_3N_4-x h (x=1, 2 and 3).

The samples with different calcining time were characterized by SEM. It can be clearly seen that the as-prepared g-C_3N_4 displayed a micrometer-size sheet-like structure (Fig. 1a). The two-step calcining samples, g-C_3N_4-x h (x=1, 2 and 3) also showed sheet-like shape, as shown in Fig. 1b-d. But, it was noteworthy that the average lateral size of thin sheets was gradually widened with increasing the calcining time.

Department of Physics, National University of Singapore, Singapore 117542. E-mail: 027wit@163.com; phyjian@nus.edu.sg

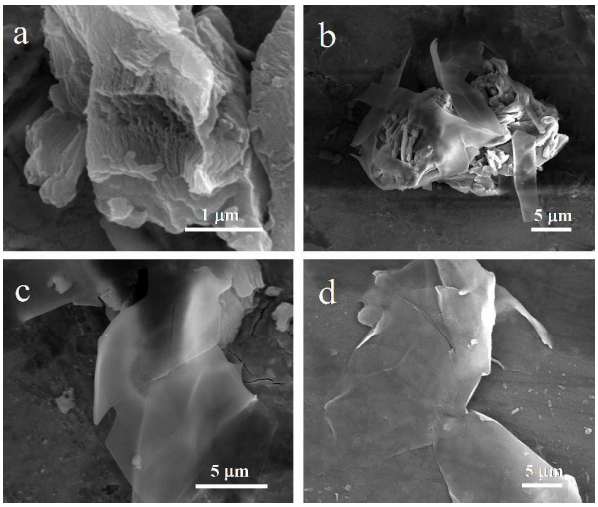

Fig. 1 SEM images of g-C_3N_4 (a), g-C_3N_4-1 h (b), g-C_3N_4-2 h (c) and g-C_3N_4-3 h (d), respectively.

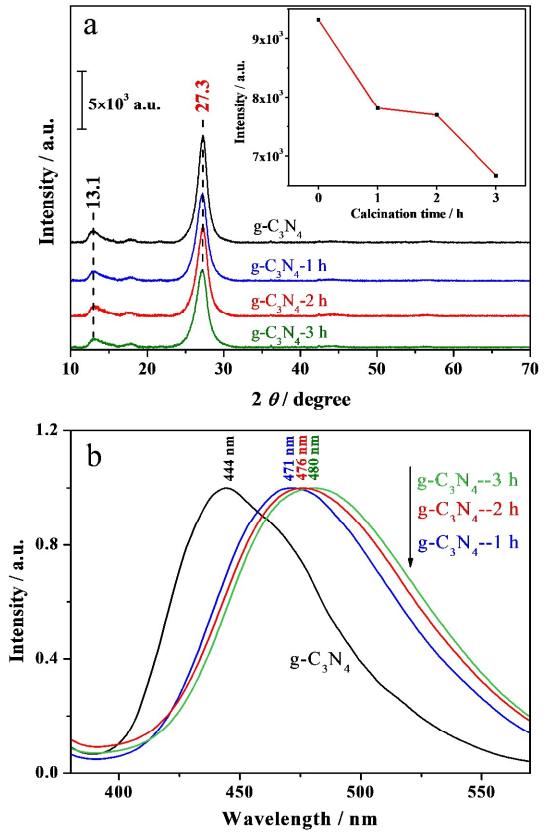

Fig. 2 XRD patterns (a) and fluorescence spectra (b) of different samples, respectively. Inset of Fig. 2a is the relationship between the peak intensity at 27.3° and calcining time.

Meanwhile, it was found that the XRD patterns of all g-C_3N_4-x h samples showed nearly identical peaks (Fig. 2a). The (002) peak θ=27.3° reflected the characteristic interlayer stacking structure, while the (100) diffraction at 13.1° indicated the interplanar structural packing.[12] In order to investigate the slight changes of the intensity of (002) diffraction, eight different batches samples with a same mass were measured under the same test conditions. For the same kind of sample, the obtained XRD patterns from eight different batches overlapped extremely well. The relative standard deviations (RSD %) of the intensity of (002) diffraction in the XRD patterns was less than 0.9%. By comparing the XRD patterns of these four samples, it was found that the intensity of (002) diffraction related to the interlayer stacking was gradually decreased with prolonged calcining time (inset of Fig. 2a), suggesting that the layer thickness became thinner. The results of SEM and XRD indicated that when the calcining time was prolonged, the average size of g-C_3N_4-x h samples became larger in x-y plane and thinner in the longitudinal direction. Fig. 2b shows the fluorescence spectra of all samples. The fluorescence spectra of the modified g-C_3N_4-x h samples were normalized by setting the peak intensity be unit at the intrinsic emission peaks. The intrinsic emission peak displayed a red-shift from 444 nm to 471, 476 and 480 nm, correspondingly. These spectral changes implied that the prolonged calcining time increased the conjugation length in the CN structure, resulting in the average lateral size of thin sheets becoming widened, well in accordance with the SEM results (Fig. 1).

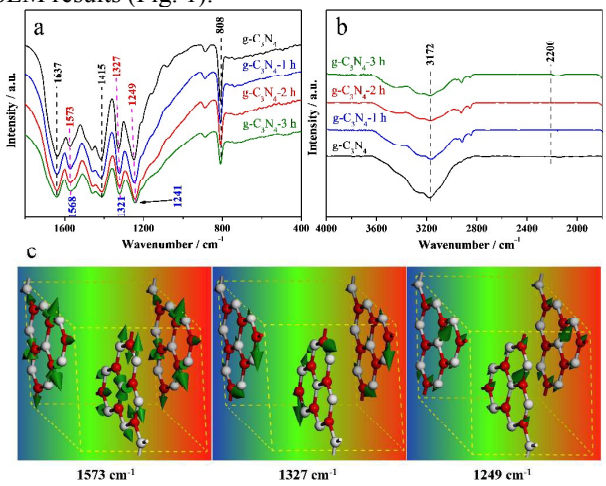

Fig. 3 FT-IR spectra (a-b) of different samples. Assignments of three vibrational modes of g-C_3N_4 within CASTEP calculations (c). Red and gray spheres represent C and N atoms, and green arrows show dipole derivative unit vectors.

FT-IR spectra of all samples are shown in Fig. 3. The absorption bands located at ~1637, 1415 and 809 cm^{-1} were originated from the C=N stretching vibration, the out-of-phase stretching vibration of N-C (sp^3) and the breathing vibration of tri-s-triazine ring,[12] respectively (Fig. 3a). And there was no any peak around 2200 cm^{-1} (-C≡N nitrile function) (Fig. 3b), which confirmed the planarity of

these materials.[13-15] By comparing the FT-IR spectra of the g-C_3N_4 and two-step calcining samples, the peaks at 1573, 1327 and 1249 cm^{-1} were respectively shifted by 5, 6 and 8 cm^{-1} toward low frequencies after the further calcining process. Based on the first principles calculations, it was found that the bands near 1573, 1327 and 1249 cm^{-1} belonged to N-C-N symmetrical stretching, asymmetrical C=N stretching and =C(sp^2) bending vibration mode, respectively (Fig. 3c). It seems possible that the shifts might be caused by the electrophilic effect of the thin layer g-C_3N_4, resulting in the weaken strength of C-N covalent bonds and the lower frequencies.[16] Moreover, comparing with g-C_3N_4, the two-step calcining samples exhibits gradually reduced absorption peak around 3172 cm^{-1} that were indicative of secondary and primary amines.[1] This observation indicated that further calcining process do not significantly disturb the local order of the polymer-like melon chains, but just speak for the formation of a more condensed polymeric network of g-C_3N_4-x h with fewer -NH_2 and -NH- motifs.

To explore the SERS activity of these samples, we compared the normal Raman spectra of g-C_3N_4-x h+Ag hybrids (Fig. 4a). Many strong characteristic peaks of g-C_3N_4 was observed in the spectrum of g-C_3N_4+Ag, and two broad peaks appeared around 1500 and 400 cm^{-1} in the spectrum of g-C_3N_4-3 h+Ag. If they were used as the SERS substrates, their own strong signal could interfere on the SERS signals of probe molecules. However, no obvious peak was observed in the normal Raman spectra of g-C_3N_4-1 h+Ag and g-C_3N_4-2 h+Ag, suggesting they may be ideal SERS substrates.

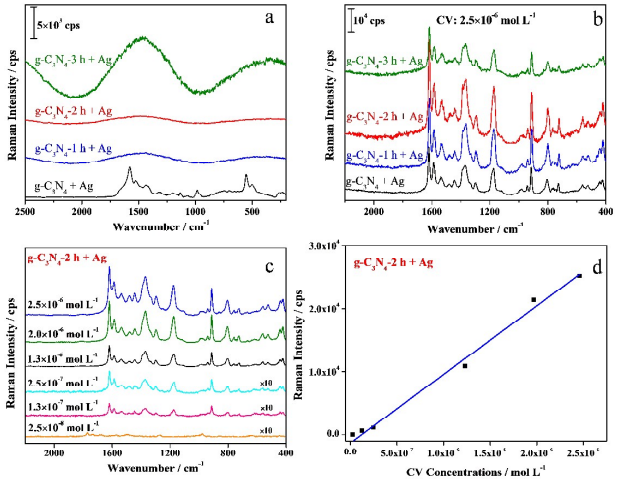

Fig. 4 Raman (a) and SERS (b) spectra on different substrates, SERS spectra of CV at different concentrations (c) and the relationship between CV concentrations and Raman intensity at 1619 cm^{-1} (d) on g-C_3N_4-2 h+Ag substrate, respectively.

Meanwhile, Fig. 4b compared the SERS spectra of CV (2.5×10^{-6} mol L^{-1}) on different substrates. Strong SERS responses and plentiful peaks of CV were observed on all substrates. Generally speaking, both electromagnetic enhancement and chemical enhancement contribute to the total SERS enhancement. Herein, in these hybrid substrates, the Ag nanoparticles immobilized on the surface and edges of modified g-C_3N_4 sheets could produce a greatly enhanced electromagnetic field ('hot spots'), leading to a dramatically enhanced Raman response of the probe molecules near the hot spots. Meanwhile, there was a chemical enhancement from the charge transfer between Raman probe molecules and Ag nanoparticles, as reported in our previous work.[11,17]

Although we have investigated the SERS response of the g-C_3N_4+Ag substrate and it provided an enhancing factor as high as 4.6×10^8 for CV in our previous work,[11] the SERS effect of g-C_3N_4+Ag was relatively poor among these four substrates in this work. Moreover, we note that the g-C_3N_4-2 h+Ag substrate provided an enhancing factor as high as 3.0×10^9, being much greater than that provide by other three substrates. This result demonstrated the strongest Raman enhancement effect on the g-C_3N_4-2 h+Ag substrate, probably due to the different morphology and formation of a more appropriate condensed polymeric network of g-C_3N_4-2 h in the two-step calcining process.

Furthermore, we investigated the SERS spectra of CV at different concentrations on g-C_3N_4-2 h+Ag (Fig. 4c), and the relationship between SERS intensity (at 1619 cm^{-1}) and the concentration of CV (Fig. 4d), which indicates that there was a wide linear response range from 2.5×10^{-8} to 2.5×10^{-6} mol L^{-1}. Therefore, the semiquantitative analysis of organic pollutants with g-C_3N_4-2 h+Ag as SERS substrates was feasible.

To gain further insight into the essential reason for the difference among the SERS activity of these four SERS substrates, the zeta potential and thermogravimetric analysis were investigated. It was found that the aqueous dispersions of g-C_3N_4 exhibited a highly negative surface charge of -20.1 mV, which was in good agreement with that reported in previous works.[12] And for the modified g-C_3N_4-x h (x=1, 2 and 3), the zeta potential of the corresponding aqueous dispersions were -22.5, -33.6 and -24.3 mV, respectively. As far as we know, the probe molecules (aromatic molecules) were strongly adsorbed on the surfaces of g-C_3N_4 sheets and the surrounding of Ag nanoparticles, due to the π-π interaction and electrostatic interaction between aromatic molecules and g-C_3N_4.[11] Hence, the modified g-C_3N_4-2 h with the highest zeta potential value can absorb more probe molecules around the surface and edges, which was beneficial to increase the concentration of probe molecules in the vicinity of the hot spots, ultimately making a highest SERS activity among the different substrates. In addition, Fig. 5 shows the thermogravimetric analysis (TGA) results of the melamine and the modified g-C_3N_4-x h (x=1, 2 and 3). The melamine

was relatively stable up to 290 °C, after which it started to decompose and lose mass. TGA curve of g-C_3N_4 revealed that it was significantly robust and nonvolatile up to 600 °C, even under air. A strong endothermal peak appeared at 630 °C (Fig. 5a), paralleled by consecutive complete weight loss, indicating thermal decomposition and complete vaporization of the fragments. And the TGA curves of the modified g-C_3N_4-x h showed some features similar to that of g-C_3N_4. Moreover, the strong endothermal peak displayed a red-shift with the prolonged calcining time (Fg. 5b). Note that the thermal stability of CN materials somewhat differs between different preparation methods, which may be due to different degree condensation and different packing motifs.[18] So the TGA results directly conformed the modified g-C_3N_4-x h with different calcining time possessed different degree of polymerization, well consistent with the FT-IR results (Fig. 3). This above discussion indicated that the minute changes in morphology and degree of polymerization could change the microstructure of modified g-C_3N_4, leading to the g-C_3N_4-2 h+Ag substrate with an almost invisible Raman response. For SERS sensing, a SERS substrate itself without any interfering peak would suggest that this substrate could possess a lower limit of detection for the probe molecules. Hence, by comparing the g-C_3N_4 and g-C_3N_4-3 h+Ag with strong Raman signals, the g-C_3N_4-2 h+Ag substrate showed a related low limit of detection and a wide linear response range, as shown in Fig. 4(c-d). In a certain sense, this result also indicated the g-C_3N_4-2 h+Ag substrate possessed a higher SERS activity. Therefore, the highest SERS activity of the g-C_3N_4-2 h+Ag substrate was partly attributed to the modified g-C_3N_4-2 h with the highest zeta potential which can be beneficial to absorb more probe molecules around the hot spots. The other possible reason for the highest SERS activity could be a minute changes in morphology and a more appropriate condensed polymeric network of g-C_3N_4-2 h, which excluded the interference of SERS substrate-self in SERS sensing.

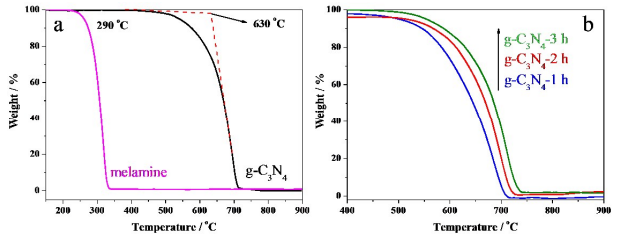

Fig. 5 Thermogravimetric analysis (TGA) results for the melamine and g-C_3N_4 (a), and different modified g-C_3N_4 substrates (b), respectively.

In conclusion, we showed a path to prepare modified g-C_3N_4 materials by a two-step calcining method. It was found that the average lateral size and the degree of polymerisation of the modified g-C_3N_4 sheets were gradually widened and lager with increasing the calcining time. Moreover, compared to the reported g-C_3N_4+Ag substrates, the modified g-C_3N_4-2 h+Ag substrates exhibited superior SERS activity. The utilization of a two-step calcining method therefore opens new opportunities for significant improvement of carbon nitride synthesis, microstructure, and SERS activity.

Preparation of modified g-C_3N_4 and SERS substrates

In brief, the g-C_3N_4 was prepared by heating melamine to 520 ^oC for 4 h under air atmosphere in a muffle furnace. Then, the as-prepared yellow powder was further calcined in a CVD furnace and held this temperature for different time. After the furnace cooling to the room temperature, a more fluffy powder was obtained. Herein, Ag nanoparticles were prepared by the NH_2OH•HCl reduction method.[17] A total of 40 mL of NaOH solution (7.5 mmol L^{-1}) was added to 50 mL of a hydroxylamine hydrochloride solution (3.0 mmol L^{-1}). Then 10 mL of $AgNO_3$ aqueous solution (10 mmol L^{-1}) was rapidly added to the above mixture under ultrasound irradiation with a powder of 140 W. After 5 min, a milky gray color colloid was obtained and stored in a refrigerator at 4 ^oC for further use. Finally, g-C_3N_4+Ag hybrids were prepared. To prepare the hybrids, the modified g-C_3N_4 powders (0.02 g) were added in 20 mL of Ag nanoparticles colloid under vigorous stirring at room temperature. After stirred for 1 h, aliquots of the mixture were transferred into 5 mL microcentrifuge tubes and centrifuged at 5000 rpm for 5 min. The precipitates from each tube were redispersed in 5 mL of Milli-Q water. The resultant dispersion was stored at ambient temperature prior to use.[11] All the chemicals were of analytical grade and were used as received. Milli-Q water (18.2 MΩ cm) provided by a Milli-Q Labo apparatus (Thermo Fischer Scientific) was used in all experiments.

Characterization

The obtained samples were analyzed by scanning electron microscope (SEM, JSM-5510LVA, Japan), X-ray diffraction (XRD, D8 Advance TXS, Germany), FT-IR spectrometer (Nicolet 6700, Thermo Fischer), and fluorescence spectrometer (FP-6200, Jasco). Raman and SERS spectra were measured on a confocal Raman spectrometer (DXR, Thermo Fischer) equipped with a diode laser of excitation of 532 nm. The measured conditions were: the laser output power: 1 mW; sample exposure times: twice; collect exposure time: 0.2 s. The geometry and IR analysis of g-C_3N_4 were performed were performed using the plane-wave ultrasoft (PWUS) pseudo-potential method as implemented in the Cambridge Sequential Total Energy Package (CASTEP) code.[19] The theoretical study was also performed using the PWUS pseudo-potential method with the generalized gradient approximation (GGA) and correlation in the Perdew-Wang 91 (PW91),[20] and with the local density approximation

(LDA) functional of Ceperley and Alder as parameterized by Perdew and Zunger (CAPZ).[21]

Notes and references

1 X. Li, J. Zhang, X. Chen, A. Fischer, A. Thomas, M. Antonietti, and X. Wang, *Chem. Mater.*, 2011, **23**, 4344-4348.
2 M. Shalom, S. Gimenez, F. Schipper, I. Herraiz-Cardona, J. Bisquert, and M. Antonietti, *Angew. Chem. Int. Ed.*, 2014, **126**, 3728-3732.
3 M. Shalom, S. Inal, C. Fettkenhauer, D. Neher and M. Antonietti., *J. Am. Chem. Soc.*, 2013, **135**, 7118-7121.
4 J. Oh, S. Lee, K. Zhang, J. O. Hwang, J. Han, G. Park, S. O. Kim, J. H. Park and S. Park, *Carbon*, 2014, **66**, 119-125.
5 X. Li, J. Chen, X. Wang, J. Sun and M. Antonietti. *J. Am. Chem. Soc.*, 2011, **133**, 8074-8077.
6 X. Chen, J. Zhang, X. Fu, M. Antonietti and X. Wang, *J. Am. Chem. Soc.*, 2009, **131**, 11658-11659.
7 X. Li, X. Wang and M. Antonietti, *ACS Catal.*, 2012, **2**, 2082-2086.
8 D. Guo, R. Shibuya, C. Akiba, S. Saji, T. Kondo and J. Nakamura, *Science*, 2016, **351**, 361-365.
9. W. Gong, J. Zou, S. Zhang, X. Zhou and J. Jiang, *Electroanalysis*, 2016, **28**, 227-234.
10 J. Zhang, X. Chen , K. Takanabe, K. Maeda, K. Domen, J. D. Epping, X. Fu, M. Antonietti and X. Wang, *Angew. Chem. Int. Ed.*, 2010, **49**, 441-444.
11 J. Jiang, L. Zhu, J. Zou, L. Ou-yang, A. Zheng and H. Tang, *Carbon*, 2015, **87**, 193-205.
12 J. Jiang, L. Ou-yang, L. Zhu, A. Zheng, J. Zou, X. Yi and H. Tang, *Carbon*, 2014, **80**, 213-221.
13 Y. Zhao, Z. Liu, W. Chu, L. Song, Z. Zhang, D. Yu, Y. Tian, S. Xie and L. Sun, *Adv. Mater.*, 2008, **20**, 1777-1781.
14 A. Pfitzmann, E. Fliedner and M. Fedtke, *Polym. Bull.*, 1994, **32**, 311-317.
15 C. Wörner and R. Mülhaupt, *Angew. Chem. Int. Ed.*, 1993, **32**, 1306-1308.
16 J. Xu, L. Zhang, R. Shi and Y. Zhu. *J. Mater. Chem. A*, 2013, **1**, 14766-14772.
17 J. Jiang, L. Ou-yang, L. Zhu, J. Zou and H. Tang, *Sci. Rep.*, 2014, **4**, 3942(1-9).
18 X. Wang, S. Blechert and M. Antonietti. *ACS Catal.* 2012, **2**, 1596-1606.
19 M. D. Segall, P. J. D. Lindan, M. J. Probert, C. J. Pickard, P. J. Hasnip, S. J. Clark and M. C. Payne, *J. Phys. Condens. Matter.*, 2002, **14**, 2717-2744.
20 J. P. Perdew and Y. Wang, *Phys. Rev. B*, 1992, **45**, 13244-13249.
21 D. M. Ceperley and B. J. Alder, *Phys. Rev. Lett.*, 1980, **45**, 566-569.

Graphical Abstract

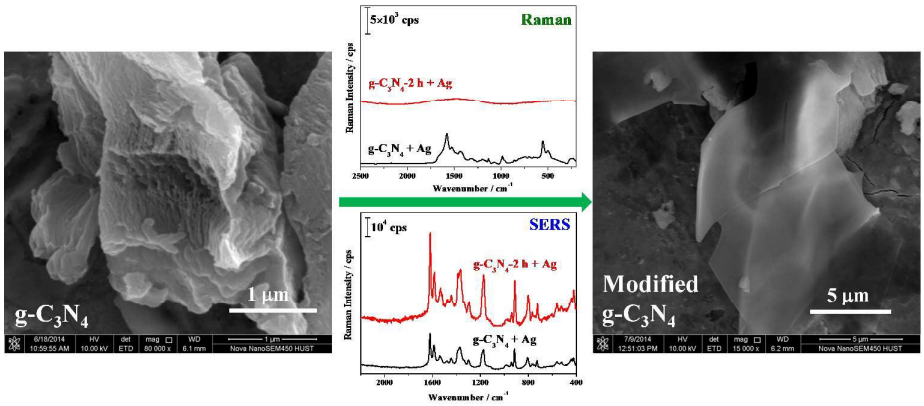

Highlights

►The modified g-C_3N_4 substrates were prepared by a two-step calcining method. ►The morphology and microstructure of modified g-C_3N_4 were successfully controlled. ►The modified g-C_3N_4-2 h+Ag hybrid substrates exhibited superior SERS activity. ►It has promising applications in routine SERS analysis of trace organic pollutants.